HAO, X., WANG, S., FAN, Y., LIU, D., LIANG, Y., ZHANG, M. and FERNANDEZ, C. 2024. A novel least squares support vector machine-particle filter algorithm to estimate the state of energy of lithium-ion battery under a wide temperature range. *Journal of energy storage* [online], 89, article number 111820. Available from: https://doi.org/10.1016/j.est.2024.111820

A novel least squares support vector machine-particle filter algorithm to estimate the state of energy of lithium-ion battery under a wide temperature range.

HAO, X., WANG, S., FAN, Y., LIU, D., LIANG, Y., ZHANG, M. and FERNANDEZ, C.

2024

A Novel Least Squares Support Vector Machine-particle Filter Algorithm to estimate the state of energy of lithium-ion battery under a wide temperature range

Xueyi Hao[a], Shunli Wang[a*b], Yongcun Fan[a], Donglei Liu[a], Yawen Liang[a], Mengyun Zhang[a], Carlos Fernandez[c]

[a]*School of Information Engineering, Southwest University of Science and Technology, Mianyang 621010, China;*

[b]*Colledge of Electrical Engineering, Sichuan University, Chengdu, 610065, China;*

[c]*School of Pharmacy and Life Sciences, Robert Gordon University, Aberdeen AB10-7GJ, UK.*

Abstract: The state of energy (SOE) is a key indicator for lithium-ion battery management systems (BMS). Based on the second-order resistance-capacitance equivalent circuit model and online parameter identification using the dynamic weights particle swarm optimization (DWPSO) method, a least-squares support vector machine-particle filter (LSSVM-PF) algorithm is proposed to construct a particle filter to estimate the SOE of a lithium-ion battery, and then transfer the resulting estimation error together with the experimentally measured voltage and current values to a trained LSSVM model, and use the LSSVM model to optimize the SOE estimates obtained by the PF algorithm twice to improve the accuracy of SOE estimation for lithium-ion batteries. The feasibility of the proposed algorithm is verified using two complex operating conditions and at three different temperatures. The validation results show that the maximum error of SOE estimation of the proposed algorithm is 0.0284 for a wide temperature range under Beijing Bus Dynamic Stress Test (BBDST) condition, and 0.0226 for a wide temperature range under Dynamic Stress Test (DST) condition. the proposed algorithm significantly improves the accuracy of SOE estimation and provides a reference for fundamental applications of lithium-ion batteries.

Keywords: Least square support vector machine, Particle filter, State of energy, Dynamic weights particle swarm optimization, Lithium-ion battery

***Corresponding author**: Shun-Li Wang. E-mail address: wangshunli@swust.edu.cn

1 Introduction

Nowadays, in the whole world, the new energy vehicle industry has become an inevitable trend for the strategic transformation of the traditional automobile industry in the future [1-3]. As an important energy storage power source for electric vehicles, the power battery is one of the keys to the development of the electric vehicle industry [4-7]. The main role of the battery management system is to monitor and record the battery temperature, voltage, current and battery capacity in real-time, provide timely feedback and deal with them, which helps to improve the efficiency of the power battery, extend its service life and guarantee the safe and stable operation of the whole battery system [8-12]. Therefore, it is necessary to build a reliable BMS and accurately estimate the battery SOE to ensure safe and efficient battery operation [13, 14].

The current research on battery SOE estimation methods is not perfect and comprehensive, and some literature on energy research is only extended based on estimated capacity without a specific analysis of energy states [15, 16]. The traditional SOE estimation algorithms are mainly divided into model-based and data-driven methods [17-22]. The literature [23] proposes a method for estimating the SOE of the battery pack based on prediction, taking into account the future voltage and temperature changes of the battery pack. The literature [24] uses a traceless particle filtering algorithm (UPF) to estimate the SOE of the battery for solving the nonlinearity problem of lithium-ion batteries, and the results show satisfactory performance in terms of accuracy and reliability. In the literature [25], it proposes a modified method based on a radial basis function (RBF) neural network to estimate the actual energy released by the recovered energy when the battery current direction is changed, and the results show that the method can effectively estimate the battery energy and improve the SOE estimation accuracy. In the literature [26], this paper proposes a novel SOE estimation method using a particle filter and extended Kalman filter, and the experimental results show that the algorithm has high accuracy and stability. The literature [27] uses a long short-term memory (LSTM) artificial neural network model and an ampere-time integration method to correct the open-circuit voltage identified online to achieve SOE estimation under dynamic operating conditions in a wide temperature range. The literature [28] proposes the use of a long short-term memory (LSTM) deep neural network to estimate both SOC and SOE and compares it with other popular algorithms to illustrate its accuracy and robustness.

Model-based state estimation usually requires the construction of an equivalent circuit model followed by parameter identification [29-31]. Commonly used equivalent circuit models include Thevenin equivalent circuit, second-order capacitance-resistance (RC) equivalent circuit model, PNGV equivalent model and so on [32-34]. Select the appropriate equivalent model, based on which the parameter identification method is studied. At present, the main parameter identification methods are offline parameter identification methods, online parameter identification methods and only parameter identification methods [35-38]. Among them, literature [39] proposed a real-time insulation resistance detection method based on the least squares method with a variable forgetting factor, and the proposed method can quickly track the change of insulation resistance under noise interference conditions. The literature [40] uses a cuckoo search optimization algorithm for model parameter identification based on a second-order RC equivalent model, and its results show that the method outperforms the standard algorithmic nonlinear least-squares method. The literature [41] constructed a PNGV model and proposed a random mutation ant colony optimization (RMACO) algorithm applicable to fractional parameter identification, using the collected voltage and current data for parameter identification of the fractional PNGV model, and finally showed that the algorithm has better parameter estimation. In the literature [42], it proposes a dual-polarized (DP) equivalent circuit model to describe two rhombic cells with different anodes, comparing the analytical equations, least-square-based methods, and heuristic algorithms used to parameterize the model, concluding that the particle swarm optimization approach is the best trade-off in terms of computational time, accuracy, and robustness.

Therefore, in this paper, a new least squares support vector machine-particle filter algorithm is proposed for energy state estimation. Firstly, a second-order RC equivalent model is constructed and a dynamic weights particle swarm optimization algorithm is proposed for parameter identification to obtain the results of parameter identification and insight into the inter-parameter law. Secondly, a particle filter is constructed for SOE estimation of lithium-ion batteries, and the obtained estimation results and estimation errors are transferred to the trained least-squares support vector machine model [43] together with the experimentally obtained voltage and current data, and the output results are used for the secondary correction of SOE estimation to improve the estimation accuracy of the particle filter.

The first chapter introduces the background and status of the current energy state of lithium batteries; the second chapter introduces the theoretical knowledge on which this paper is based, including the establishment of the equivalent model, the introduction of the dynamic weights particle swarm optimization algorithm and the usage of parameter identification, the principle of the least squares support vector machine algorithm, and the overall framework and ideas of the least squares support vector machine-particle filtering algorithm; the third chapter describes the comparison and analysis of the results based on the proposed algorithm with other existing algorithms over a wide temperature range and under different complex operating conditions; the fourth section concludes the paper by demonstrating the superiority and limitations of the proposed algorithm.

2 Mathematical

2.1 Second-order RC equivalent model

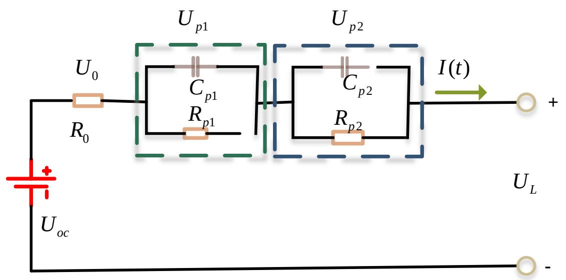

Figure 1 Second-order RC equivalent model

As shown in Figure 1, the second-order RC equivalent model is obtained by adding an RC parallel loop to the Thevenin model. In the figure, the RC loop composed of R_{p1} and C_{p1} represents the stage of rapid voltage change during the chemical reaction inside the battery; the RC loop is composed of R_{p2} and C_{p2} represents the stage of slow voltage change during the chemical reaction inside the battery. The simple model is easy to calculate, but cannot accurately describe the operating characteristics of the battery. The complex model can better characterize the charging and discharging characteristics of the battery, but the calculation volume will be greatly increased, which reduces the adaptability and generalization of the model. The effects of different orders of equivalent circuit models on the SOE estimation effect are compared, among which, the second-order RC equivalent model has higher accuracy, and the computational effort is a bit larger than that of Thevenin and PNGV models, but it is within the acceptable range. Taking this into account, this paper decides to use the second-order RC equivalent model for SOE estimation. According to Kirchhoff's current law as well as the voltage law, equation (1) can be obtained.

$$\begin{cases} U_L = U_{oc} - i(t)R_0 - U_{p1} - U_{p2} \\ \dfrac{dU_{p1}}{dt} = -\dfrac{U_{p1}}{R_{p1}C_{p1}} + \dfrac{i}{C_{p1}} \\ \dfrac{dU_{p2}}{dt} = -\dfrac{U_{p2}}{R_{p2}C_{p2}} + \dfrac{i}{C_{p2}} \end{cases} \tag{1}$$

In equation (1), Uoc represents the terminal voltage, R_0 represents the internal resistance of the second-order RC equivalent model, while R_{p1}, R_{p2} represent the polarization resistance, C_{p1}, C_{p2} represent the polarization capacitance, and U_{p1}, U_{p2} refer to the voltages of the two RC loops, respectively.

2.2 Dynamic weighted particle swarm optimization algorithm

Parameter identification methods include offline identification methods, online identification methods and intelligent identification methods. Considering the advantages and disadvantages of several identification methods, we choose to use the PSO [44, 45] algorithm of intelligent methods as the basic algorithm for parameter identification. At present, the PSO algorithm has been widely used in function optimization, neural network training, pattern assignment, fuzzy control and other fields. However, the PSO algorithm also has defects such as poor local search ability, easy falling into local extrema, and low search accuracy. Therefore, the improvement of the PSO algorithm becomes a key challenge. In order to eliminate the limitation of particle velocity boundary and accelerate the convergence of the PSO algorithm, Clerc et al. introduced the compression factor into the basic PSO algorithm, and the introduction of the compression factor can change the velocity of particles. Although the PSO algorithm after adding the compression factor achieves the balance between global search and local search to a certain extent, the solution details of the problem change as the number of iterations increases, and the fixed value has many defects in the overall solution process. Thus, changing inertia weights are introduced to dynamically adapt to the problem-solving process. Thus, a new DWPSO algorithm is proposed in this paper, and its flow chart is shown in Figure 2.

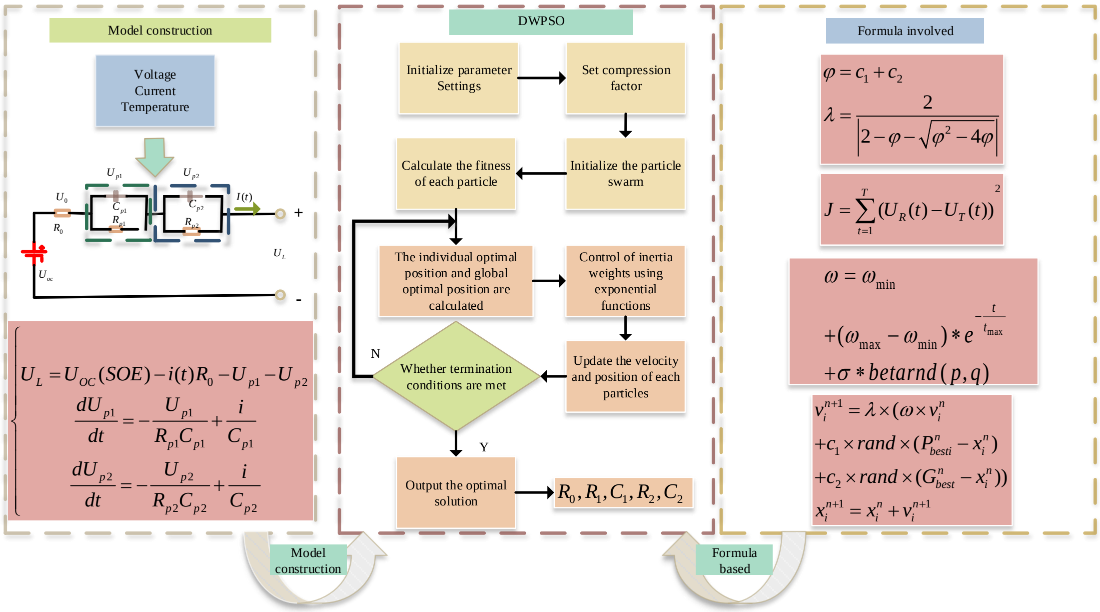

Figure 2 Parameter identification flow chart

As shown in Figure 2, this paper further optimizes the particle swarm optimization algorithm after adding the compression factor, and adopts an improved strategy of dynamic adjustment of inertia weights based on the CFPSO algorithm, using an exponential function to control the change of weights ω, with the increase of iteration number $e^{-\frac{t}{t_{max}}}$ nonlinearly decreases, $betarnd$ is a random number generator in $matlab$ can Generate random numbers that conform to the beta distribution, which can increase the global search ability of the algorithm in the late iteration of the algorithm and reduce the possibility of the algorithm falling into local last, the improved inertia weight expression is shown in Equation (2).

$$\omega = \omega_{min} + (\omega_{max} - \omega_{min}) * e^{-\frac{t}{t_{max}}} + \sigma * betarnd(p, q) \tag{2}$$

where t is the current iteration number and t_{max} is the maximum iteration number; σ is the inertia adjustment factor, taken as 0.1; ω_{max} is the initial inertia weight, taken as 0.9; ω_{min} is the inertia weight at the maximum iteration number of the algorithm, taken as 0.4; $p = 1, q = 3$.

2.3 Least Squares Support Vector Machine

There is a contradiction between the network structure of a neural network and the generalization ability of its network; the more complex the network, the better the fit to existing samples but the weaker the generalization ability to unknown samples; while the network is too simple, it is difficult to find patterns from a limited number of samples. It is because of this contradiction that neural network models often reach the predefined training goal, while their estimation of unknown samples remains unsatisfactory. With the development of statistical learning theory, support vector machine (SVM) provides new ideas to alleviate this contradiction, especially in the solution of small samples and nonlinear prediction problems that show strong generalization ability.

Support vector machine is a binary classification model, and its basic model is a linear classifier defined on the feature space with maximum interval, and the maximum interval makes it different from a perceptron; SVM also includes kernel tricks, which makes it a substantially nonlinear classifier. Support vector machines, as one of the mainstream machine learning algorithms at present, are widely used in many fields of life, such as medicine, control, and mechanical troubleshooting. The algorithm has an outstanding ability in solving nonlinear and high-dimensional conditions, so support vector machines are mainly used to study loud classification and regression. the learning strategy of SVM is interval maximization, which can be formalized as a problem of solving convex quadratic programming, which is also equivalent to the problem of minimizing a regularized hinge loss function. the learning algorithm of SVM is the optimization algorithm for solving convex quadratic programming.

The SVM algorithm is a supervised data-driven learning algorithm, which has been commonly used in the fields of pattern discrimination, data categorization and regression prediction. Based on VC dimension theory and minimization of structural risk theory, the SVM algorithm uses the hyperplane obtained from the optimal partitioning theory to turn the classification and regression problem of sample data into a quadratic programming problem and then finds the global optimal solution with good accuracy and generalization ability, which is a comprehensive data-driven algorithm with excellent performance. The schematic diagram of support vector regression is shown in Figure 3.

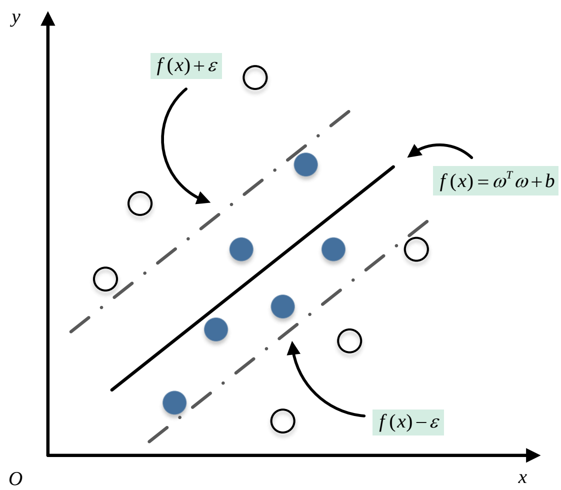

Figure 3 Support vector regression diagram

A support vector machine can obtain the relationship between the inputs and outputs of an unknown system based on a given set of sample data. When a set of inputs is re-given, the support vector machine can then estimate the output of that system as accurately as possible.

The least squares support vector machine (LSSVM) is an optimization algorithm for the SVM algorithm. The experimentally measured voltage and current data are used as the original input, and the second-order RC equivalent model is used as the basis for parameter identification using the adaptive particle swarm algorithm described above to obtain the five parameters that make the fitness function optimal. The model parameters obtained from the parameter identification are applied to the constructed particle filter for SOE estimation. Then, the SOE estimates and SOE estimation errors obtained by the particle filter, together with the SOE estimates obtained by the ansatz integration method and the experimentally measured voltage values, are used as the input to the LSSVM model, and the output is the SOE estimation error value. To ensure the accuracy of the constructed model, part of the filtered data of the PF algorithm is used as training data for the construction of the LSSVM model. The completed LSSVM model is trained to effectively correct the initial prediction value obtained by the PF algorithm using the error compensation of the model output, which in turn ensures the robustness and generalization of the algorithm while obtaining a more accurate SOE prediction value, fully realizing the superiority of the combined algorithm.

2.4 LSSVM-PF based on DWPSO parameter identification algorithm

SOE is an important part of the research on lithium-ion batteries. SOE reflects the deterioration degree of batteries and is a state parameter representing the remaining battery life and remaining power of lithium-ion batteries. Its definition is shown in equation (3).

$$SOE(k+1) = SOE(k) + \frac{\int_{k}^{k+1} \eta P(k) dk}{E_T} \tag{3}$$

In equation (3), $SOE\ (k+1)$ represents the energy status value of the next moment, $SOE\ (k)$ represents the energy status value of the current moment, $P\ (k)$ is the power of the lithium-ion battery, E_T is the rated energy of the battery, η is the charging and discharging efficiency of lithium-ion batteries.

The PF algorithm has the phenomenon of "particle degradation", which seriously limits the estimation accuracy of SOE. As a typical data-driven algorithm, the SVM algorithm is theoretically based on the optimal risk structure of the sample data, effectively avoiding the problems of overfitting and dimensional catastrophe, and maintaining good generalization performance while taking into account the accuracy of the prediction information and the complexity of the approximation function. Moreover, the feature of being sensitive to only some key samples ensures that the SVM algorithm has high robustness.

In this paper, the filtered data of the PF algorithm is selected as the sample data for constructing the LSSVM algorithm model, and the PF filtered estimates are optimized by the good regression prediction performance of LSSVM to further reduce the estimation error of LSSVM, to achieve the purpose of improving the estimation accuracy. The specific combined algorithm flow chart is shown in Figure 4. For the construction of the LSSVM model, it is crucial to select the appropriate inputs and outputs.

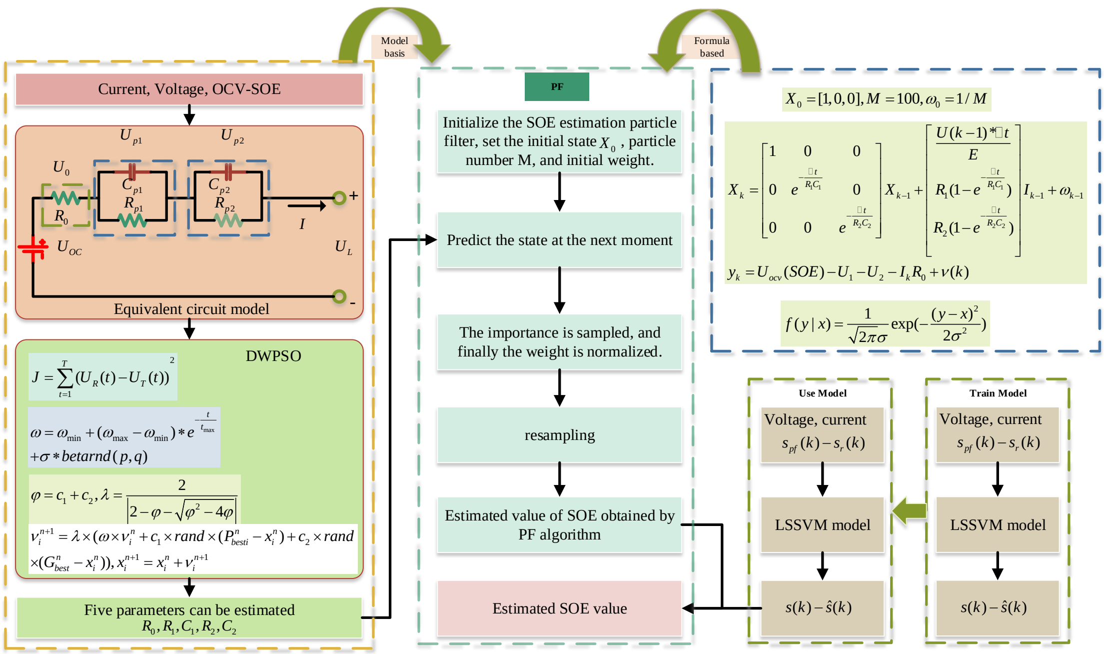

Figure 4 LSSVM-PF algorithm flow chart

As shown in Figure 4, $s(k) - \hat{s}(k)$ represents the error compensation obtained after the output of the LSSVM model, and is added to the SOE estimate obtained by the PF algorithm to obtain a more accurate SOE estimate after quadratic optimization.

Considering that the model is required to have a good adaptability to the actual working conditions of the battery and the complexity of the actual working conditions, the training data sources are finally set as BBDST working conditions and DST working conditions data. In order to better describe the dynamic characteristics of battery charging and discharging process, current, voltage and other signals are necessary. Finally, the LSSVM model with four inputs and one output is constructed. The input includes current, voltage, SOE estimate of PF at k time, SOE estimate error of PF, and SOE estimate of ampere-hour integral, and the output is the prediction error of PF. In order to ensure the accuracy of the model, part of the filter data in PF algorithm is used as training data to build the LSSVM model.

In the LSSVM model, the input PF SOE estimation error value is the error value obtained simply by using the PF algorithm for SOE estimation, while the output error compensation value of the LSSVM model is the estimated error value after the LSSVM model training, which is used to compensate the estimated value of PF to improve the estimation accuracy of the PF algorithm.

In order to ensure the accuracy of the model, some filtering data in PF algorithm is used as training data to construct LSSVM model. The number of iterations and error threshold are set as the mark of the completion of the model construction, and then the validation data is used to verify the validity of the established model. The trained LSSVM model uses the error compensation of the model output to effectively correct the initial predicted value obtained by the PF algorithm, and the sum of the two is very good for the SOE quadratic estimate, thus ensuring the robustness and generalization of the algorithm and obtaining the SOE predicted value with higher accuracy, fully realizing the superiority of the combined algorithm.

3 Experiment

To verify the effectiveness of the proposed estimation method for estimating the energy state of lithium-ion batteries, this chapter will experimentally analyze the parameter identification results under the adaptive particle swarm algorithm and the energy state estimation under the least squares support vector machine-particle filter algorithm, and verify the effectiveness of the proposed algorithm for energy state estimation under different lithium-ion battery test conditions.

3.1 Experimental platform

Lithium-ion battery test experiments are an important method to obtain battery data and verify the estimation of battery state parameters. To obtain accurate experimental data for SOE estimation and verification, this paper uses a large multiplier power cell charge/discharge test equipment to test the lithium-ion battery under complex operating conditions. The battery test experiment platform used in this paper is shown in Figure 5.

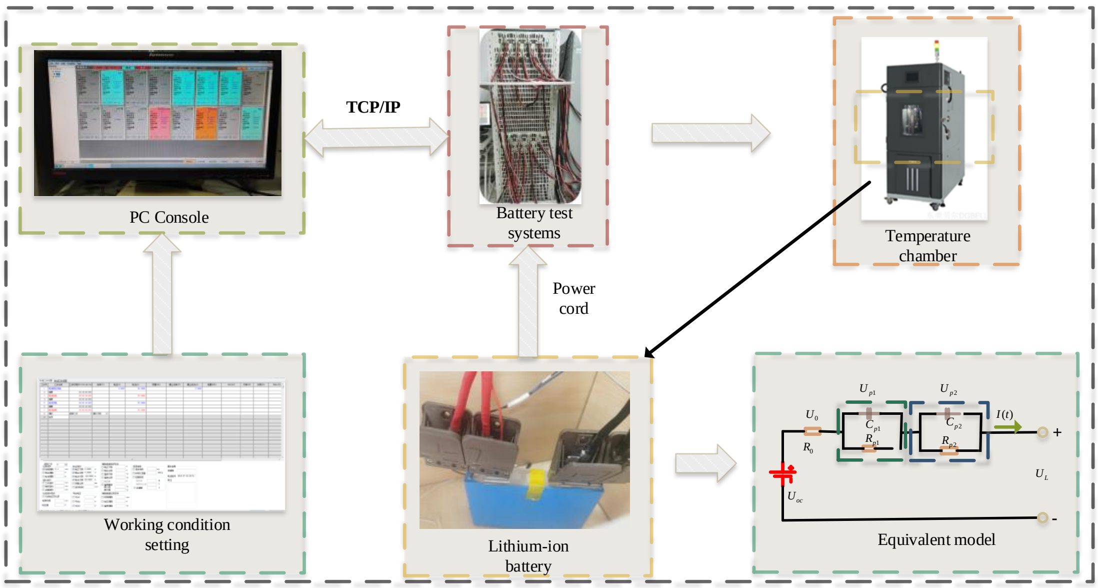

Figure 5 Schematic diagram of the experimental platform

As shown in Figure 5, the experimental test platform mainly consists of the power battery large rate charge/discharge tester (BTS 750-200-100-4), three-layer independent temperature-controlled high and low-temperature test chamber (BTT-331C), etc. During the experiment, the upper computer is used to set the test conditions, while real-time monitoring of battery status and collection of experimental data. The function of the three-layer independent high and low-temperature thermostat is to control the temperature of the power lithium battery during the test experiment, which can accurately simulate the complex natural environment of low temperature, high temperature, high temperature and high humidity, low temperature and low humidity, etc. This paper takes the ternary lithium battery as the research object, whose rated capacity is 72Ah.

First of all, the battery is charged to the full charge state in the way of constant current and constant voltage, and the cycle step is started after 40 minutes, until the battery terminal voltage reaches the lower limit of the cut-off voltage. The cut-off condition of constant current and constant voltage charging is that the current drops to 0.05C and the discharge cut-off voltage is 2.75V. A BBDST working cycle is 300s in total, which mainly includes 19 working steps such as starting, accelerating, accelerating, sliding, braking, etc., which can well simulate the actual working situation of the power lithium battery. Therefore, this working condition is used to evaluate the state of the power lithium battery for experimental verification.

3.2 Parameter identification Result

To verify the accuracy of the DWPSO algorithm described above, parameter identification of the constructed equivalent circuit model was performed using the BBDST and DST test conditions at 5°C, 25°C and 35°C, respectively. The experiments were conducted with a ternary lithium battery, and the measured voltage was compared with the voltage obtained from the parameter identification results of the DWPSO algorithm to verify the accuracy of the DWPSO algorithm, and the parameter identification results obtained from the PSO and CFPSO algorithms were compared with the DWPSO algorithm to verify the effectiveness and superiority of the DWPSO algorithm. The results are shown in Figure 6.

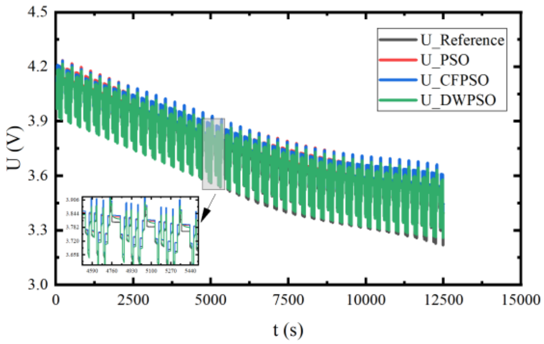

(a) Voltage contrast curve at 5 degrees

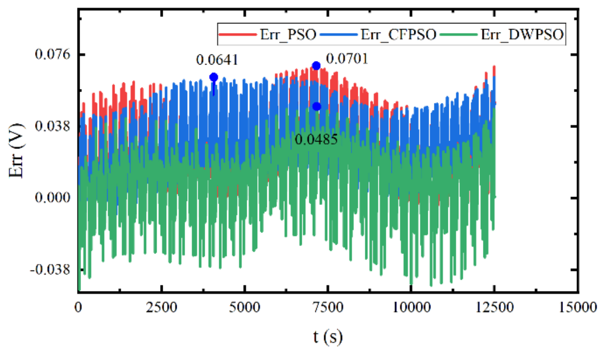

(b) Voltage error results at 5 degrees

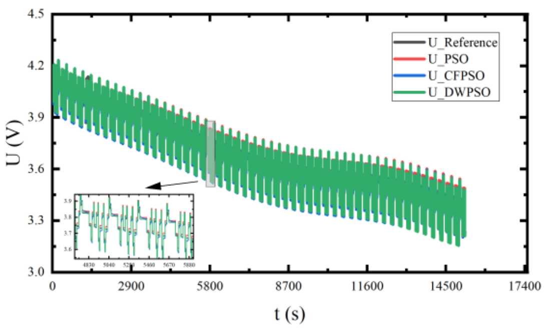

(c) Voltage contrast curve at 25 degrees

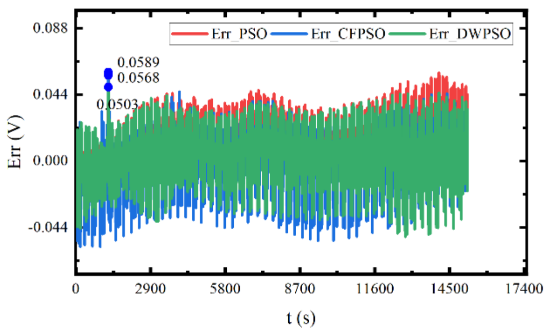

(d) Voltage error results at 25 degrees

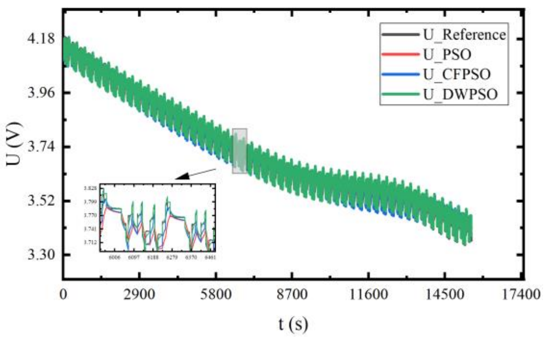

(e) Voltage contrast curve at 35 degrees

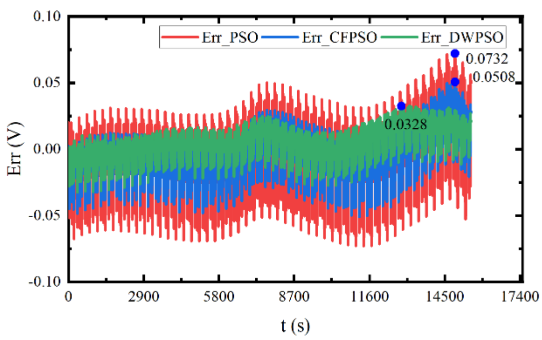

(f) Voltage error results at 35 degrees

Figure 6 Parameter identification results under BBDST working condition

As shown in Figure 6, Figure 6(a), Figure 6(c) and Figure 6(e) show the comparison of the experimentally measured voltage at 5°C, 25°C and 35°C under BBDST conditions with the fitted voltage obtained from the PSO algorithm identification, the fitted voltage obtained from the CFPSO algorithm identification and the fitted voltage obtained from the DWPSO algorithm identification, respectively. Figure 6(b), Figure 6(d) and Figure 6(f) show the error profiles corresponding to the above three plots, respectively. According to the comparison results of the simulated voltage and the experimentally measured voltage, it is clear that the simulated terminal voltage of the parameters obtained based on the DWPSO parameter identification method is closer to the experimentally measured terminal voltage. The root mean square error (RMSE), mean absolute error (MAE) and maximum error (MaxE) of the simulated voltage with different temperature parameter identification under BBDST conditions are shown in Figure 7.

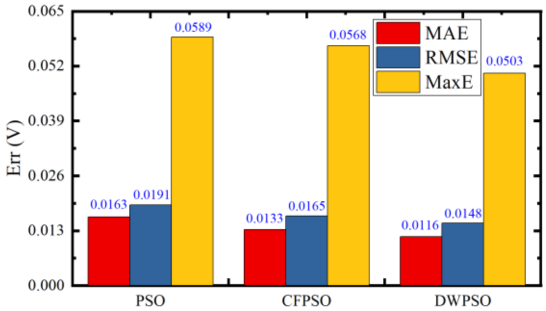

(a) Parameter identification algorithm performance index at 25 degrees

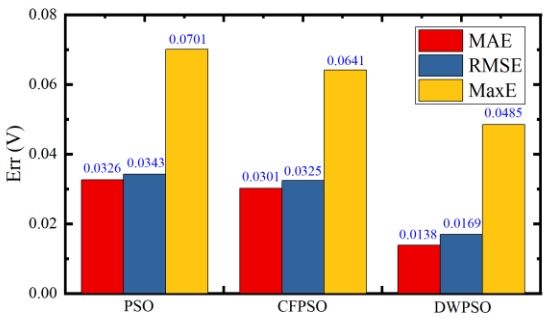

(b) Parameter identification algorithm performance index at 5 degrees

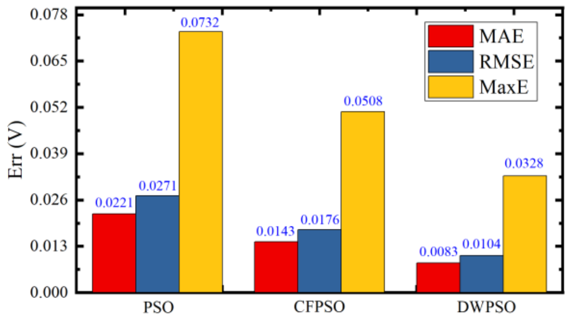

(c) Parameter identification algorithm performance index at 35 degrees

Figure 7 Performance index of each parameter identification algorithm under BBDST working condition

In Figure 7, MAE and RMSE are the two most commonly used metrics to measure the accuracy of variables and are also two important yardsticks for evaluating the models. MAE represents the mean value of the absolute error between the predicted and observed values, while RMSE is expressed as the sample standard deviation of the difference between the predicted and observed values, and to indicate the degree of dispersion of the sample, and MaxE is the maximum error value of the algorithm. From the figure, it can be seen that MAE, RMSE and MaxE under the DWPSO algorithm are smaller than the CFPSO algorithm and PSO algorithm, and the DWPSO parameter identification algorithm has a high accuracy of parameter identification.

To further verify the recognition effect of the DWPSO algorithm, the DST working conditions were tested under the temperature conditions of 5℃, 25℃ and 35℃ respectively, and the parameter recognition results under this working condition are shown in Figure 8.

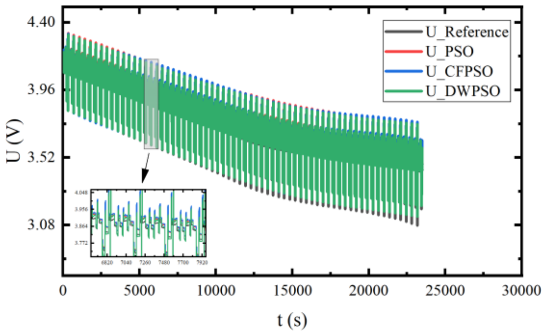

(a) Voltage contrast curve at 5 degrees

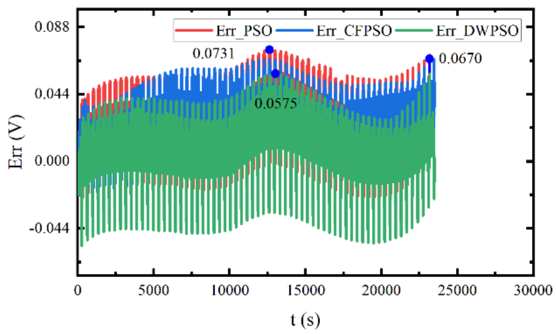

(b) Voltage error results at 5 degrees

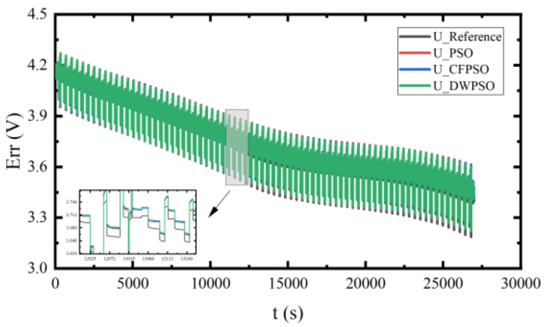

(c) Voltage contrast curve at 25 degrees

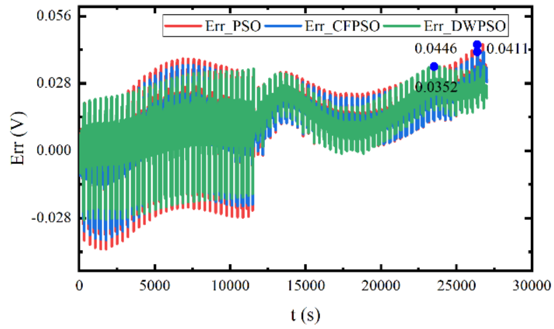

(d) Voltage error results at 25 degrees

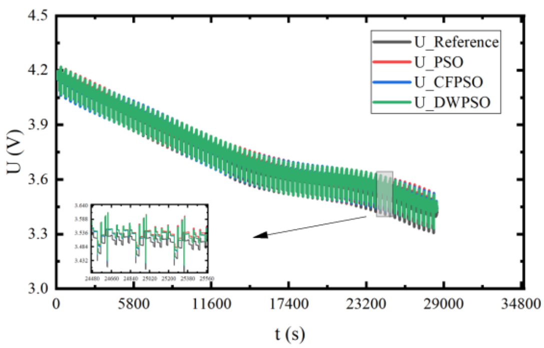

(e) Voltage contrast curve at 35 degrees

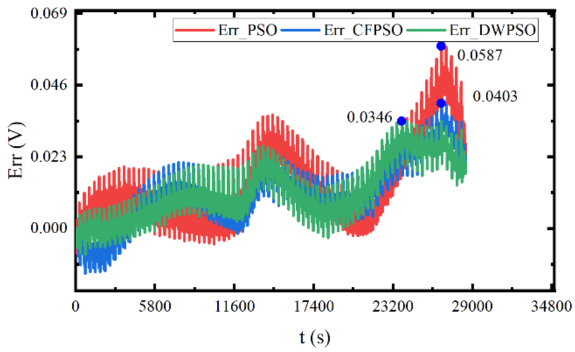

(f) Voltage error results at 35 degrees

Figure 8 Parameter identification results under DST working condition

From the comparison of the simulated voltages of different parameter identification methods with the experimentally measured voltages at different temperatures and their error results, it can be obtained that the simulated voltages obtained by the DWPSO algorithm are more closely matched with the experimentally measured voltages, and the maximum error is 57.5mV at 5℃, 35.2mV at 25℃, and 34.6mV at 35℃. Figure 9 shows the performance index of each parameter identification method under DST conditions.

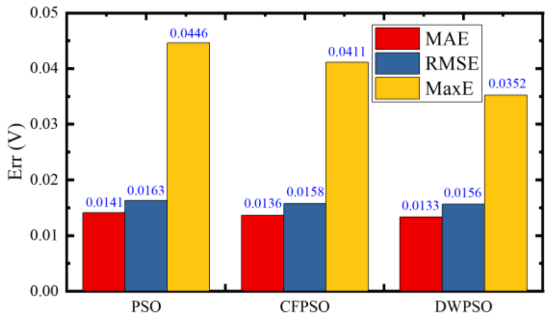

(a) Parameter identification algorithm performance index at 25 degrees

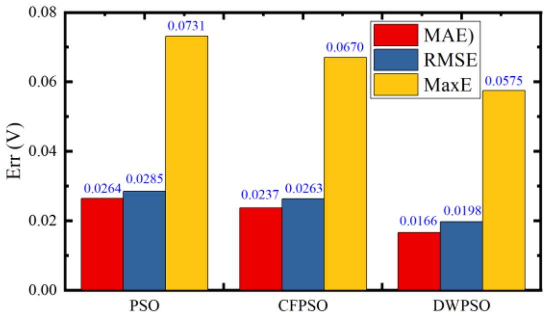

(b) Parameter identification algorithm performance index at 5 degrees

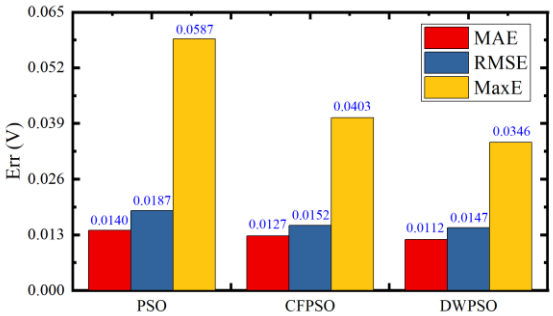

(c) Parameter identification algorithm performance index at 35 degrees

Figure 9 Performance index of each parameter identification algorithm under DST working condition

From the results depicted in the figure, the MAE, RMSE and MaxE of the DWPSO parameter identification method are the smallest among the three parameter identification algorithms at different temperatures, thus reflecting the high identification accuracy of the DWPSO algorithm.

The simulation results of BBDST and DST conditions show that the DWPSO algorithm can identify the parameters of the constructed second-order RC equivalent circuit model of lithium-ion battery very well, and according to the comparison of three parameter identification algorithms, the PSO algorithm has the worst identification effect due to the disadvantages of easy to fall into the local optimal solution and poor convergence accuracy. Compared with the

CFPSO algorithm, the DWPSO algorithm further optimizes the problems of the PSO algorithm and can better realize the lithium-ion battery model parameter identification.

3.3 Experimental analysis under BBDST working condition

In this paper, the experimental data obtained from the BBDST working condition experiments at different temperatures are used to verify the adopted SOE estimation algorithm based on LSSVM-PF, and the SOE estimation results under the LSSVM algorithm and PF algorithm are compared and analyzed with the SOE estimation results under LSSVM-PF, to illustrate the effectiveness of the LSSVM-PF algorithm for SOE estimation. The SOE estimation results under BBDST working conditions are shown in Figure 10.

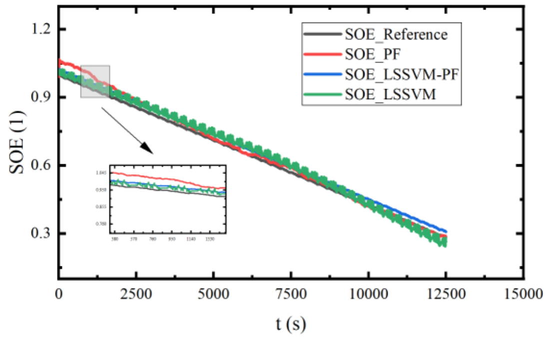

(a) Comparison of SOE estimation results at 5 degrees

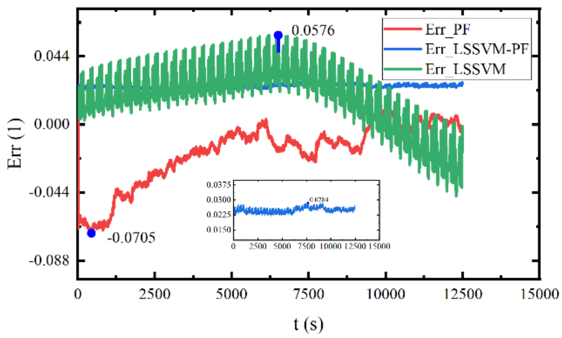

(b) SOE estimation error curve at 5 degrees

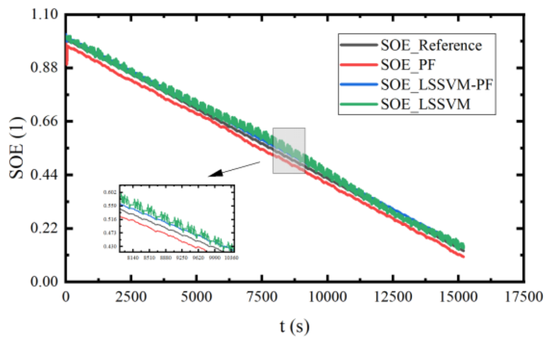

(c) Comparison of SOE estimation results at 25 degrees

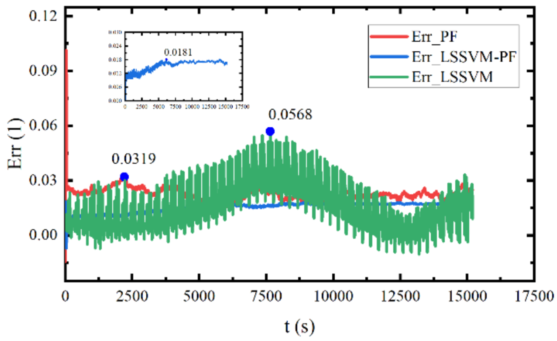

(d) SOE estimation error curve at 25 degrees

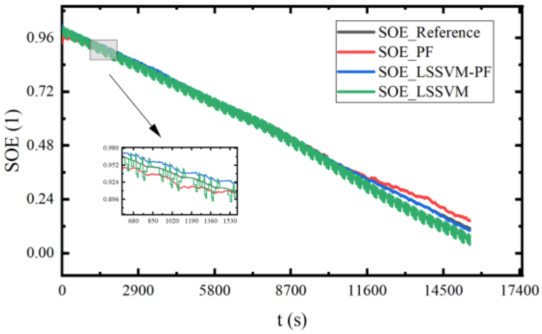

(e) Comparison of SOE estimation results at 35 degrees

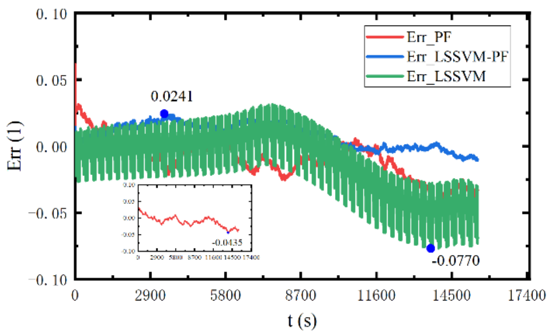

(f) SOE estimation error curve at 35 degrees

Figure 10 SOE estimation curve and error curve of each algorithm under BBDST working condition

Figure 10 shows the SOE estimation results and SOE estimation errors for the BBDST conditions at 5°C, 25°C and 35°C. The reference value of SOE is the estimated value of SOE obtained by the ampere-hour integral method. From the SOE estimation error curves at the three temperatures, we can see the estimation effect of the three algorithms on SOE, and it can be concluded that the LSSVM-PF algorithm used in this paper has the best estimation effect on SOE, and the estimation curve fits better with the experimental result curve, and its corresponding error curve has a more gentle overall trend, and the comparison with the error curves of other algorithms can be concluded that the LSSVM-PF algorithm The LSSVM-PF algorithm has better convergence and good stability. And the proposed algorithm takes less time in running time, so it can be seen that the proposed algorithm has higher computational efficiency. The performance indexes of several algorithms are listed in Figure 11.

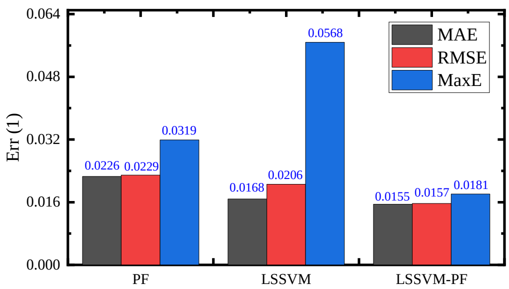

(a) Performance metrics of each SOE estimation algorithm at 25 degrees

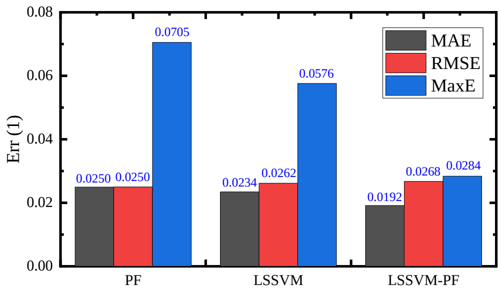

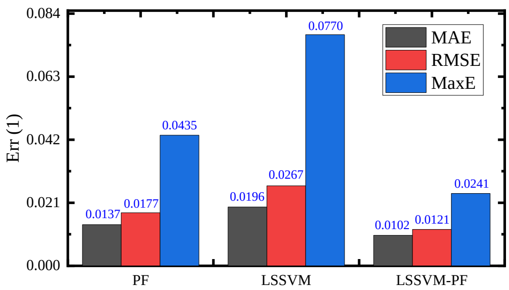

(b) Performance metrics of each SOE estimation algorithm at 5 degrees

(c) Performance metrics of each SOE estimation algorithm at 35 degrees

Figure 11 Performance metrics of each SOE estimation algorithm under BBDST operating conditions

In Figure 11, the MAE, RMSE, and MaxE of the LSSVM-PF algorithm at 25°C are 0.0155, 0.0157, and 0.0181, respectively; the MAE, RMSE, and MaxE of the algorithm at 5°C are 0.0192, 0.0268, and 0.0284, respectively; and the MAE, RMSE, and MaxE of the algorithm at 35°C are 0.0102, 0.0121, and 0.0241, respectively. The experimental results show that the LSSVM algorithm can secondarily optimize the SOE results of the PF algorithm to a certain extent, and its estimation effect is better than that of the PF filter algorithm estimation alone and the LSSVM algorithm alone, therefore, the LSSVM-PF algorithm can better achieve the SOE estimation of lithium-ion batteries.

The BP neural network algorithm, as one of the data-driven algorithms, can also be used to optimize the estimates of the PF algorithm, and the proposed algorithm is compared with the BP-PF algorithm and the BP algorithm to obtain the SOE estimates of several algorithms for the BBDST operating conditions at different temperatures as shown in Figure 12.

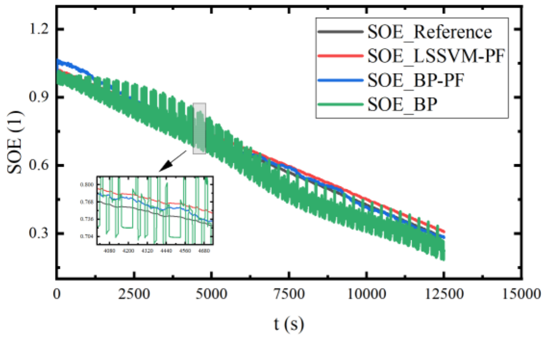

(a) Comparison of SOE estimation results at 5 degrees

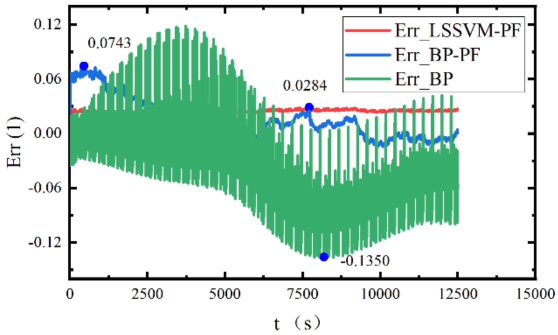

(b) SOE estimation error curve at 5 degrees

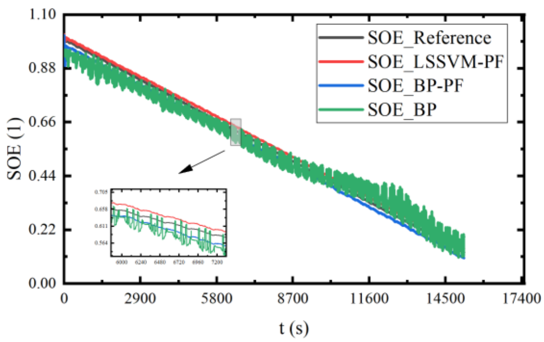

(c) Comparison of SOE estimation results at 25

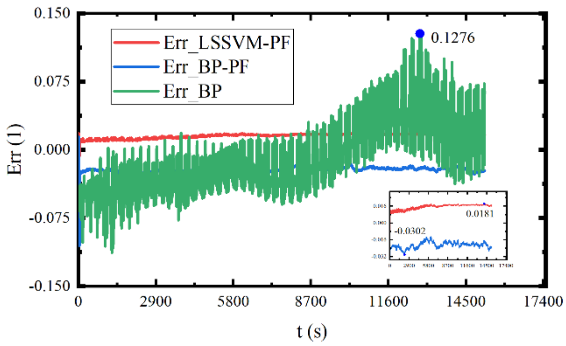

(d) SOE estimation error curve at 25 degrees

degrees

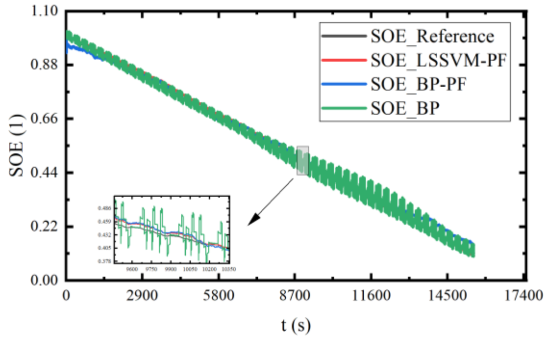

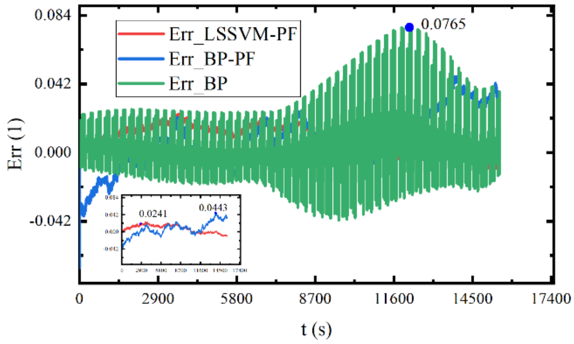

(e) Comparison of SOE estimation results at 35 degrees

(f) SOE estimation error curve at 35 degrees

Figure 12 SOE estimation curves and error curves of the proposed algorithm and other algorithms under BBDST working conditions

The six figures in Figure 12 clearly show the comparison of the SOE estimation results between the LSSVM-PF algorithm and the BP-PF algorithm-BP algorithm at 5°C, 25°C, and 35°C for the BBDST operating conditions. The performance comparison between the proposed algorithm and the other two algorithms under BBDST conditions is shown in Table 1.

Table 1 Performance metrics of the proposed algorithm with other algorithms for SOE estimation under BBDST operating conditions

Algorithm	Temperature	MAE	RMSE	MaxE
LSSVM-PF	5	0.0192	0.0268	0.0284
	25	0.0155	0.0157	0.0181
	35	0.0102	0.0121	0.0241
BP-PF	5	0.0191	0.0265	0.0742
	25	0.0211	0.0215	0.0302
	35	0.0142	0.0183	0.0443
BP	5	0.0558	0.0648	0.1350
	25	0.0318	0.0376	0.1276
	35	0.0115	0.0172	0.0758

The performance indexes of the proposed algorithm and other algorithms at different temperatures under BBDST conditions are listed one by one in Table 1. Through the comparison of several performance indicators, it can be analyzed that the MAE and RMSE values of the

LSSVM-PF algorithm are smaller than the other two algorithms, which indicates that the LSSVM algorithm has the ability of quadratic optimization for the PF algorithm to estimate SOE due to the BP algorithm. Therefore, the LSSVM-PF algorithm can estimate the SOE well in a wide temperature range under BBDST conditions.

3.4 Experimental analysis under DST working condition

The DST condition is a complex condition after the simplification of the U.S. federal city operating condition, which is important to verify the SOE estimation effect of the algorithm. To further test the estimation effect of the LSSVM-PF algorithm for SOE estimation, the DST working conditions were tested on ternary lithium batteries with a rated capacity of 72Ah at 5℃, 25℃ and 35℃, respectively, and the LSSVM-PF algorithm was applied to estimate the SOE value of lithium-ion batteries. The results of SOE estimation under the DST condition are shown in Figure 13.

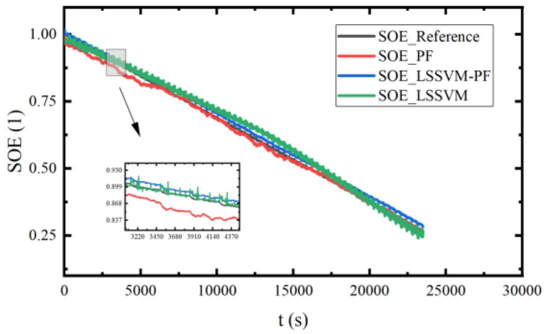

(a) Comparison of SOE estimation results at 5 degrees

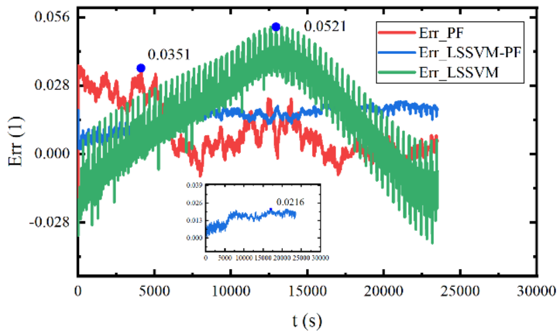

(b) SOE estimation error curve at 5 degrees

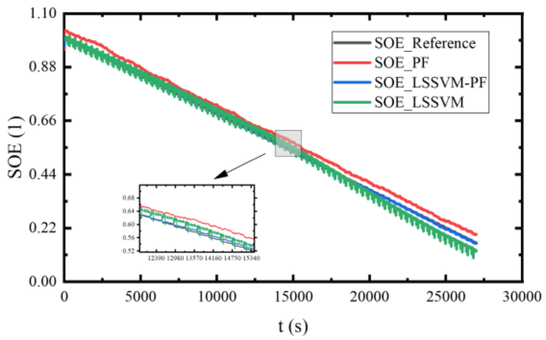

(c) Comparison of SOE estimation results at 25 degrees

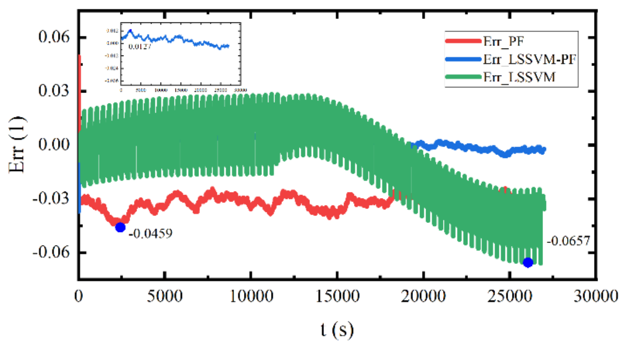

(d) SOE estimation error curve at 25 degrees

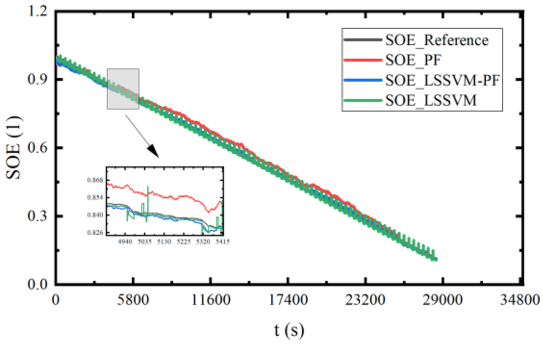

(e) Comparison of SOE estimation results at 35 degrees

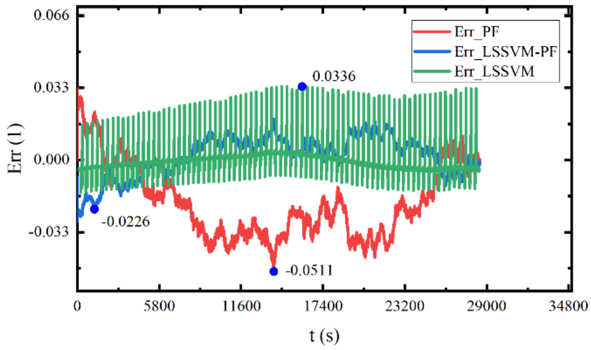

(f) SOE estimation error curve at 35 degrees

Figure 13 SOE estimation curve and error curve of each algorithm under DST working condition

As shown in Figure 13, it can be seen that the estimation error curves of the LSSVM algorithm for SOE at the three temperatures are easy to diverge, indicating the poor convergence of the LSSVM algorithm, and the estimation error curves of the PF algorithm for SOE fluctuate greatly, indicating that the stability of the PF algorithm is poor compared with the proposed algorithm, while the estimation error curves of the LSSVM-PF algorithm for SOE are relatively flat, reflecting that the LSSVM- PF algorithm has good stability and convergence, and has better estimation results. The performance indexes of several algorithms are shown in Figure 14.

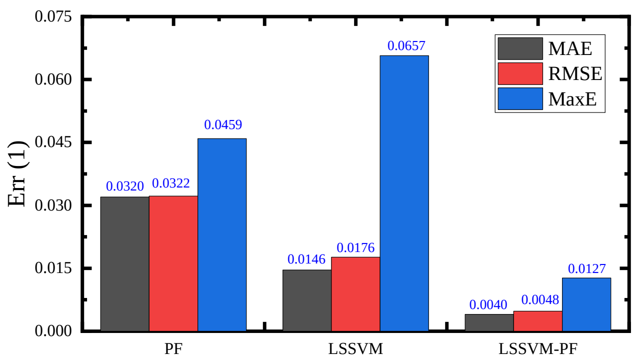

(a) Performance metrics of each SOE estimation algorithm at 25 degrees

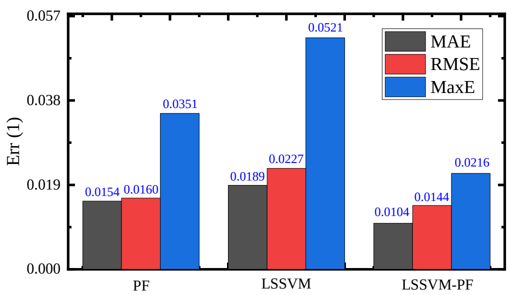

(b) Performance metrics of each SOE

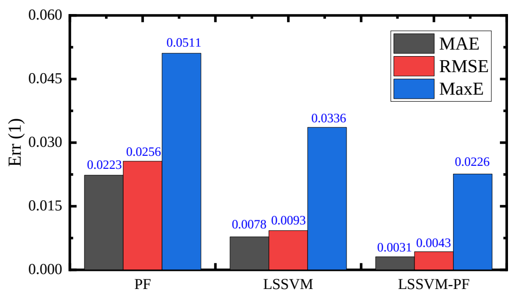

(c) Performance metrics of each SOE

estimation algorithm at 5 degrees　　　　estimation algorithm at 35 degrees

Figure 14 Performance metrics of each SOE estimation algorithm under DST conditions

From Figure 14, it can be seen that the LSSVM-PF algorithm has the smallest values of all three performance metrics, indicating the effectiveness of the LSSVM-PF algorithm for SOE estimation. By comparing several performance indexes of SOE estimation with the PF algorithm and LSSVM algorithm, it can be seen that the LSSVM-PF algorithm also has a better SOE estimation effect than the other two algorithms under DST conditions, and the secondary optimization of the estimation results of PF algorithm by using LSSVM algorithm can improve the SOE estimation accuracy of lithium-ion battery.

The same test of the proposed algorithm and the other two algorithms for estimating the SOE of the lithium-ion battery in the wide temperature range was carried out under the DST condition, and the test results are shown in Figure 15.

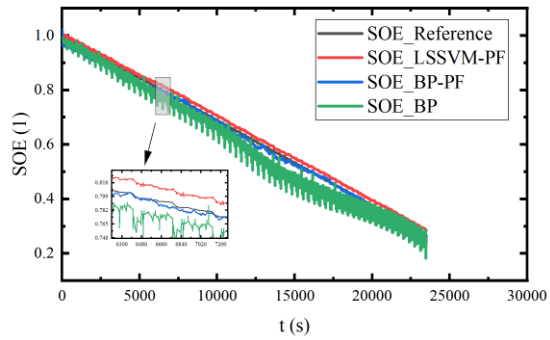

(a) Comparison of SOE estimation results at 5 degrees

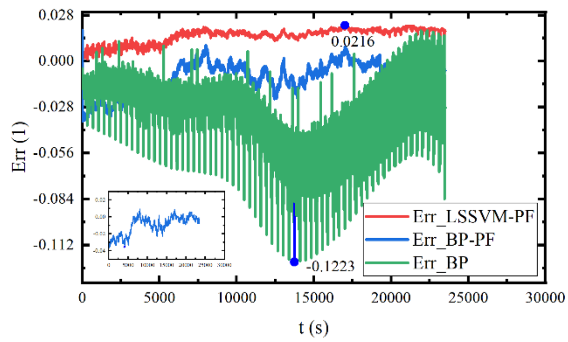

(b) SOE estimation error curve at 5 degrees

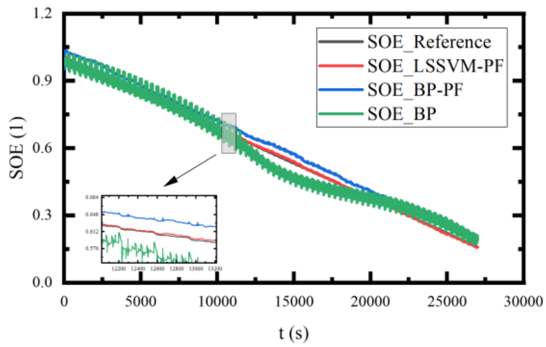

(c) Comparison of SOE estimation results at 25 degrees

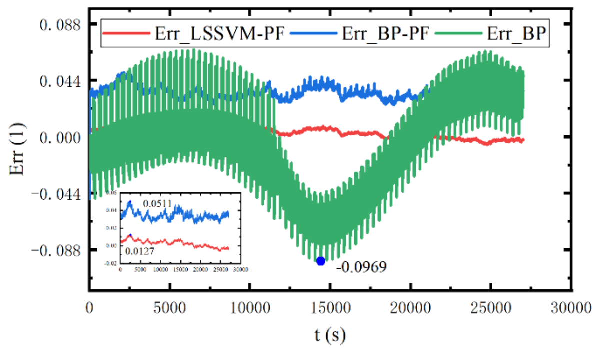

(d) SOE estimation error curve at 25 degrees

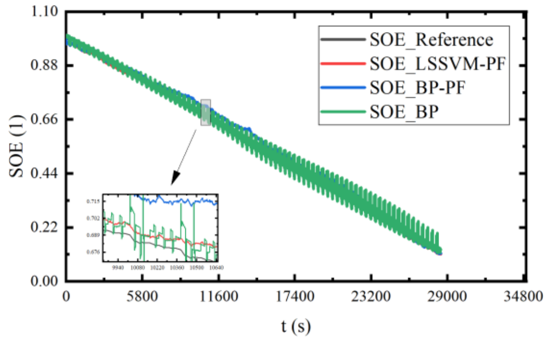

(e) Comparison of SOE estimation results at 35 degrees

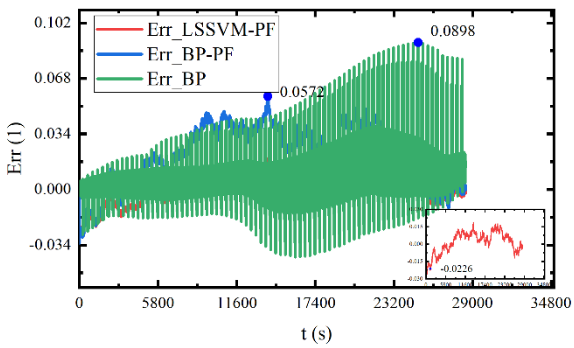

(f) SOE estimation error curve at 35 degrees

Figure 15 SOE estimation curves and error curves of the proposed algorithm and other algorithms under DST working conditions

In Figure 15, three of the result curves show that the SOE estimation curves obtained by the LSSVM-PF algorithm fit the experimentally measured curves most closely at different temperatures. The other three error profiles illustrate that the SOE estimation curves obtained by the LSSVM-PF algorithm have the smallest error values between the experimentally measured curves at different temperatures, and the stability of the algorithm is superior compared to the other two algorithms. The performance indexes of the proposed algorithm are compared with the other two algorithms in Table 2.

Table 2 Performance metrics of SOE estimation of the proposed algorithm with other algorithms under DST working condition

Algorithm	Temperature	MAE	RMSE	MaxE
LSSVM-PF	5	0.0104	0.0144	0.0216
	25	0.0040	0.0048	0.0127
	35	0.0031	0.0043	0.0226
BP-PF	5	0.0106	0.0146	0.0353
	25	0.0337	0.0340	0.0511
	35	0.0243	0.0280	0.0571
BP	5	0.0257	0.0311	0.1223
	25	0.0264	0.0341	0.0969
	35	0.0133	0.0173	0.0894

Table 2 calculates the values of each performance index for the proposed algorithm and the other two algorithms at 5°C, 25°C and 35°C under DST conditions, respectively. Through the comparison, it is clearly seen that the performance indexes of the LSSVM-PF algorithm are the best among the three algorithms at different temperatures, which illustrates the effectiveness of the LSSVM-PF algorithm for SOE estimation and improves the estimation accuracy of SOE estimation for lithium-ion batteries. It is shown that the LSSVM-PF algorithm can estimate the SOE of lithium-ion batteries well in a wide temperature range under DST conditions.

4 Conclusion

To achieve an accurate estimation of SOE, this paper proposes a DWPSO parameter identification method based on the constructed second-order RC equivalent model, which effectively optimizes the PSO algorithm and overcomes, to a certain extent, the defects of the PSO algorithm in terms of poor convergence accuracy and easy to fall into local optimal solutions. The algorithm can accurately characterize the battery, and the maximum simulation error of voltage is 57.5mV, which is smaller than that of CFPSO and PSO algorithms. For SOE estimation, the optimized LSSVM algorithm is used in this paper to optimize the SOE estimation results of the PF algorithm twice, which effectively improves the estimation accuracy of the SOE estimation and can improve the problem of large estimation errors caused by particle degradation of the PF algorithm. The results show that the maximum error of SOE estimation by the LSSVM-PF algorithm is 0.0284 under the BBDST condition, and 0.0226 under the DST condition, which is 55.77% better than that of SOE estimation by the PF algorithm. Compared with the PF algorithm, the algorithm proposed in this paper effectively improves the accuracy of SOE estimation. However, the LSSVM-PF algorithm also has some limitations. In the future, we will study the methods to reduce the computational power of the LSSVM-PF algorithm, further solve the problem of the lack of particle diversity in the PF algorithm, and will realize the method of joint estimation of SOC and SOE for lithium-ion batteries.

Acknowledgments

The work was supported by the National Natural Science Foundation of China (No. 62173281).

Reference

[1]. Wang, M.Z., et al., *State of Charge Estimation of LiFePO4 in Various Temperature Scenarios.* Batteries-Basel, 2023. **9**(1).

[2]. Wang, Z.L., et al., *A novel method of parameter identification and state of charge estimation for lithium-ion battery energy storage system.* Journal of Energy Storage, 2022. **49**.

[3]. Guo, R.H. and W.X. Shen, *A Model Fusion Method for Online State of Charge and State of Power Co-Estimation of Lithium-Ion Batteries in Electric Vehicles.* Ieee Transactions on Vehicular Technology, 2022. **71**(11): p. 11515-11525.

[4]. Laadjal, K. and A.J.M. Cardoso, *A review of supercapacitors modeling, SoH, and SoE estimation methods: Issues and challenges.* International Journal of Energy Research, 2021. **45**(13): p. 18424-18440.

[5]. Hou, E.G., et al., *Research on State of Power Estimation of Echelon-Use Battery Based on Adaptive Unscented Kalman Filter.* Symmetry-Basel, 2022. **14**(5).

[6]. Li, R., et al., *State of Charge Prediction Algorithm of Lithium-Ion Battery Based on PSO-SVR Cross Validation.* Ieee Access, 2020. **8**: p. 10234-10242.

[7]. Zhu, J., et al., *RUL Prediction of Lithium-Ion Battery Based on Improved DGWO-ELM Method in a Random Discharge Rates Environment.* Ieee Access, 2019. **7**: p. 125176-125187.

[8]. Mei, P., et al., *A Learning-Based Vehicle-Cloud Collaboration Approach for Joint Estimation of State-of-Energy and State-of-Health.* Sensors, 2022. **22**(23).

[9]. Zhang, S.Z., N. Peng, and X.W. Zhang, *A variable multi-time-scale based dual estimation framework for state-of-energy and maximum available energy of lithium-ion battery.* International Journal of Energy Research, 2022. **46**(3): p. 2876-2892.

[10]. Song, S.X., C. Fei, and H.Y. Xia, *Lithium-Ion Battery SOH Estimation Based on XGBoost Algorithm with Accuracy Correction.* Energies, 2020. **13**(4).

[11]. Xu, W., et al., *A Multi-Timescale Estimator for Lithium-Ion Battery state of Charge and State of Energy Estimation Using Dual H infinity Filter.* Ieee Access, 2019. **7**: p. 181229-181241.

[12]. Shrivastava, P., et al., *Model-based state of X estimation of lithium-ion battery for electric vehicle applications.* International Journal of Energy Research, 2022. **46**(8): p. 10704-10723.

[13]. Zhou, H.W., et al., *State-of-electrode (SOE) analytics of lithium-ion cells under overdischarge extremes.* Energy Storage Materials, 2023. **54**: p. 60-74.

[14]. Zhang, S.Z. and X.W. Zhang, *Joint estimation method for maximum available energy and state-of-energy of lithium-ion battery under various temperatures.* Journal of Power Sources, 2021. **506**.

[15]. Zhang, S.Z. and X.W. Zhang, *A novel non-experiment-based reconstruction method for the relationship between open-circuit-voltage and state-of-charge/state-of-energy of lithium-ion battery.* Electrochimica Acta, 2022. **403**.

[16]. Shrivastava, P., et al., *Comprehensive co-estimation of lithium-ion battery state of charge, state of energy, state of power, maximum available capacity, and maximum available energy.* Journal of Energy Storage, 2022. **56**.

[17]. Xueyi, H., et al., *An improved forgetting factor recursive least square and unscented particle filtering algorithm for accurate lithium-ion battery state of charge estimation.*

Journal of Energy Storage, 2023. **59**.
[18]. Zhang, S.Z. and X.W. Zhang, *A novel low-complexity state-of-energy estimation method for series-connected lithium-ion battery pack based on "representative cell" selection and operating mode division.* Journal of Power Sources, 2022. **518**.
[19]. Yang, X., et al., *A novel fuzzy adaptive cubature Kalman filtering method for the state of charge and state of energy co-estimation of lithium-ion batteries.* Electrochimica Acta, 2022. **415**.
[20]. Liu, B.Y., et al., *State of charge estimation for lithium-ion batteries based on improved barnacle mating optimizer and support vector machine.* Journal of Energy Storage, 2022. **55**.
[21]. Fan, T.E., et al., *Simultaneously estimating two battery states by combining a long short-term memory network with an adaptive unscented Kalman filter.* Journal of Energy Storage, 2022. **50**.
[22]. Song, Q.Q., et al., *A Novel Joint Support Vector Machine - Cubature Kalman Filtering Method for Adaptive State of Charge Prediction of Lithium-Ion Batteries.* International Journal of Electrochemical Science, 2021. **16**(8).
[23]. An, F.L., et al., *State of Energy Estimation for Lithium-Ion Battery Pack via Prediction in Electric Vehicle Applications.* Ieee Transactions on Vehicular Technology, 2022. **71**(1): p. 184-195.
[24]. Chang, J.Q., M.S. Chi, and T. Shen, *Model based state-of-energy estimation for LiFePO4 batteries using unscented particle filter.* Journal of Power Electronics, 2020. **20**(2): p. 624-633.
[25]. He, P., et al., *A SOE estimation method for lithium batteries considering available energy and recovered energy.* Proceedings of the Institution of Mechanical Engineers Part D-Journal of Automobile Engineering, 2023. **237**(1): p. 273-290.
[26]. Lai, X., et al., *A novel method for state of energy estimation of lithium-ion batteries using particle filter and extended Kalman filter.* Journal of Energy Storage, 2021. **43**.
[27]. Li, X.Y., et al., *Multi-state joint estimation for a lithium-ion hybrid capacitor over a wide temperature range.* Journal of Power Sources, 2020. **479**.
[28]. Ma, L., C. Hu, and F. Cheng, *State of Charge and State of Energy Estimation for Lithium-Ion Batteries Based on a Long Short-Term Memory Neural Network.* Journal of Energy Storage, 2021. **37**.
[29]. Zhang, Z.F., et al., *Estimation of state-of-energy for lithium batteries based on dual adaptive particle filters considering variable current and noise effects.* International Journal of Energy Research, 2021. **45**(11): p. 15921-15935.
[30]. Yang, S.C., et al., *A parameter adaptive method for state of charge estimation of lithium-ion batteries with an improved extended Kalman filter.* Scientific Reports, 2021. **11**(1).
[31]. Bian, X.L., et al., *A Two-Step Parameter Optimization Method for Low-Order Model-Based State-of-Charge Estimation.* Ieee Transactions on Transportation Electrification, 2021. **7**(2): p. 399-409.
[32]. Zhou, S.D., et al., *Adaptive model parameter identification for lithium-ion batteries based on improved coupling hybrid adaptive particle swarm optimization- simulated annealing method.* Journal of Power Sources, 2021. **482**.
[33]. Shrivastava, P., et al., *Combined State of Charge and State of Energy Estimation of*

Lithium-Ion Battery Using Dual Forgetting Factor-Based Adaptive Extended Kalman Filter for Electric Vehicle Applications. Ieee Transactions on Vehicular Technology, 2021. **70**(2): p. 1200-1215.
[34]. Jarrraya, I., et al., *Comparison study between hybrid Nelder-Mead particle swarm optimization and open circuit voltage-Recursive least square for the battery parameters estimation.* Journal of Energy Storage, 2022. **50**.
[35]. Wei, X., et al., *Unscented Particle Filter Based State of Energy Estimation for LiFePO4 Batteries Using an Online Updated Model.* International Journal of Automotive Technology, 2022. **23**(2): p. 503-510.
[36]. Qian, K.F., et al., *Modified dual extended Kalman filters for SOC estimation and online parameter identification of lithium-ion battery via modified gray wolf optimizer.* Proceedings of the Institution of Mechanical Engineers Part D-Journal of Automobile Engineering, 2022. **236**(8): p. 1761-1774.
[37]. Lai, X., et al., *A joint state-of-health and state-of-energy estimation method for lithium-ion batteries through combining the forgetting factor recursive least squares and unscented Kalman filter.* Measurement, 2022. **205**.
[38]. Zhang, S.Z. and X.W. Zhang, *A comparative study of different online model parameters identification methods for lithium-ion battery.* Science China-Technological Sciences, 2021. **64**(10): p. 2312-2327.
[39]. Chen, Z., et al., *A New Method of Insulation Detection on Electric Vehicles Based on a Variable Forgetting Factor Recursive Least Squares Algorithm.* Ieee Access, 2021. **9**: p. 73590-73607.
[40]. Duru, K.K., et al., *Equivalent Circuit Model Parameters Estimation of Lithium-Ion Batteries Using Cuckoo Search Algorithm.* Journal of the Electrochemical Society, 2022. **169**(12).
[41]. Jiang, Z.Y., et al., *Fractional modeling and parameter identification of lithium-ion battery.* Ionics, 2022. **28**(9): p. 4135-4148.
[42]. Kalogiannis, T., et al., *Comparative Study on Parameter Identification Methods for Dual-Polarization Lithium-Ion Equivalent Circuit Model.* Energies, 2019. **12**(21).
[43]. Li, R., W.R. Li, and H.N.A. Zhang, *State of Health and Charge Estimation Based on Adaptive Boosting integrated with particle swarm optimization/support vector machine (AdaBoost-PSO-SVM) Model for Lithium-ion Batteries.* International Journal of Electrochemical Science, 2022. **17**(2).
[44]. Xu, C.L., et al., *Surface Defects Detection and Identification of Lithium Battery Pole Piece Based on Multi-Feature Fusion and PSO-SVM.* Ieee Access, 2021. **9**: p. 85232-85239.
[45]. Li, R., et al., *On-Line Estimation Method of Lithium-Ion Battery Health Status Based on PSO-SVM.* Frontiers in Energy Research, 2021. **9**.